

# Supercontinuum generation in submicrometer diameter silica fibers

Rafael R. Gattass<sup>1</sup>, Geoffrey T. Svacha<sup>1</sup>, Limin Tong<sup>2</sup> and Eric Mazur<sup>1</sup>

<sup>1</sup> Department of Physics and Division of Engineering and Applied Sciences, Harvard University, 9 Oxford Street, Cambridge, Massachusetts 02138

<sup>2</sup> State Key Laboratory of Modern Optical Instrumentation, Zhejiang University, Hangzhou 310027, People's Republic of China

[mazur@physics.harvard.edu](mailto:mazur@physics.harvard.edu)

<http://mazur-www.harvard.edu>

**Abstract:** Silica nanowires provide strong mode confinement in a cylindrical silica-core/air-cladding geometry and serve a model system for studying nonlinear propagation of short optical pulses inside fibers. We report on the fiber diameter dependence of the supercontinuum generated by femtosecond laser pulses in silica fiber tapers with average diameters in the range of 200 nm to 1200 nm. We observe a strong diameter-dependence of the spectral broadening, which can be attributed to the fiber's diameter-dependent dispersion and nonlinearity. The short interaction length (less than 20 mm) and the low energy threshold for supercontinuum generation (about 1 nJ) make tapered fibers with diameters between 400 nm and 800 nm an ideal source of coherent white-light source in nanophotonics.

©2006 Optical Society of America

**OCIS codes:** (190.4370) Nonlinear optics, fibers; (190.5530) Pulse propagation and solitons; (320.7140) Ultrafast processes in fibers

---

## References and links

1. R. R. Alfano, and S. L. Shapiro, "Emission In Region 4000 To 7000 Å Via 4-Photon Coupling In Glass," *Phys. Rev. Lett.* **24**, 584-587 (1970).
2. R. R. Alfano, *The Supercontinuum laser source* (Springer-Verlag, New York, 1989).
3. J. C. Knight, T. A. Birks, P. S. Russell, and D. M. Atkin, "All-silica single-mode optical fiber with photonic crystal cladding," *Opt. Lett.* **21**, 1547-1549 (1996).
4. J. C. Knight, T. A. Birks, P. S. J. Russell, and D. M. Atkin, "All-silica single-mode optical fiber with photonic crystal cladding: Errata," *Opt. Lett.* **22**, 484-485 (1997).
5. P. Dumais, F. Gonthier, S. Lacroix, J. Bures, A. Villeneuve, P. G. J. Wigley, and G. I. Stegeman, "Enhanced self-phase modulation in tapered fibers," *Opt. Lett.* **18**, 1996-1998 (1993).
6. Y. K. Lize, E. C. Magi, V. G. Ta'eed, J. A. Bolger, P. Steinvurzel, and B. J. Eggleton, "Microstructured optical fiber photonic wires with subwavelength core diameter," *Opt. Express* **12**, 3209-3217 (2004).
7. J. K. Ranka, R. S. Windeler, and A. J. Stentz, "Visible continuum generation in air-silica microstructure optical fibers with anomalous dispersion at 800 nm," *Opt. Lett.* **25**, 25-27 (2000).
8. T. A. Birks, W. J. Wadsworth, and P. S. Russell, "Supercontinuum generation in tapered fibers," *Opt. Lett.* **25**, 1415-1417 (2000).
9. M. A. Foster, and A. L. Gaeta, "Ultra-low threshold supercontinuum generation in sub-wavelength waveguides," *Opt. Express* **12**, 3137-3143 (2004).
10. S. G. Leon-Saval, T. A. Birks, W. J. Wadsworth, P. S. J. Russell, and M. W. Mason, "Supercontinuum generation in submicron fibre waveguides," *Opt. Express* **12**, 2864-2869 (2004).
11. E. C. Magi, H. C. Nguyen, and B. J. Eggleton, "Air-hole collapse and mode transitions in microstructured fiber photonic wires," *Opt. Express* **13**, 453-459 (2005).
12. L. M. Tong, R. R. Gattass, J. B. Ashcom, S. L. He, J. Y. Lou, M. Y. Shen, I. Maxwell, and E. Mazur, "Subwavelength-diameter silica wires for low-loss optical wave guiding," *Nature* **426**, 816-819 (2003).
13. G. Brambilla, V. Finazzi, and D. J. Richardson, "Ultra-low-loss optical fiber nanotapers," *Opt. Express* **12**, 2258-2263 (2004).
14. L. M. Tong, J. Y. Lou, and E. Mazur, "Single-mode guiding properties of subwavelength-diameter silica and silicon wire waveguides," *Opt. Express* **12**, 1025-1035 (2004).
15. L. Provino, J. M. Dudley, H. Maillotte, N. Grossard, R. S. Windeler, and B. J. Eggleton, "Compact broadband continuum source based on microchip laser pumped microstructured fibre," *Electron. Lett.* **37**, 558-560 (2001).

16. S. Coen, A. H. L. Chau, R. Leonhardt, J. D. Harvey, J. C. Knight, W. J. Wadsworth, and P. S. J. Russell, "Supercontinuum generation by stimulated Raman scattering and parametric four-wave mixing in photonic crystal fibers," *J. Opt. Soc. Am. B* **19**, 753-764 (2002).
17. J. M. Dudley, L. Provino, N. Grossard, H. Maillotte, R. S. Windeler, B. J. Eggleton, and S. Coen, "Supercontinuum generation in air-silica microstructured fibers with nanosecond and femtosecond pulse pumping," *J. Opt. Soc. Am. B* **19**, 765-771 (2002).
18. L. Tong, J. Lou, Z. Ye, G. T. Svacha, and E. Mazur, "Self-modulated taper drawing of silica nanowires," *Nanotechnology* **16**, 1445 (2005).
19. M. Sumetsky, Y. Dulashko, and A. Hale, "Fabrication and study of bent and coiled free silica nanowires: Self-coupling microloop optical interferometer," *Opt. Express* **12**, 3521-3531 (2004).
20. M. A. Foster, K. D. Moll, and A. L. Gaeta, "Optimal waveguide dimensions for nonlinear interactions," *Opt. Express* **12**, 2880-2887 (2004).
21. M. A. Foster, J. M. Dudley, B. Kibler, Q. Cao, D. Lee, R. Trebino, and A. L. Gaeta, "Nonlinear pulse propagation and supercontinuum generation in photonic nanowires: experiment and simulation," *Appl. Phys. B* **81**, 363-367 (2005).
22. G. P. Agrawal, *Nonlinear fiber optics* (Academic Press, San Diego, 2001).
23. F. Lu, and W. H. Knox, "Generation, characterization, and application of broadband coherent femtosecond visible pulses in dispersion micromanaged holey fibers," *J. Opt. Soc. Am. B* **23**, 1221-1227 (2006).
24. J. Herrmann, U. Griebner, N. Zhavoronkov, A. Husakou, D. Nickel, J. C. Knight, W. J. Wadsworth, P. S. J. Russell, and G. Korn, "Experimental evidence for supercontinuum generation by fission of higher-order solitons in photonic fibers," *Phys. Rev. Lett.* **88**, 173901 (2002).
25. L. Tartara, I. Cristiani, and V. Degiorgio, "Blue light and infrared continuum generation by soliton fission in a microstructured fiber," *Appl. Phys. B* **77**, 307-311 (2003).
26. I. Cristiani, R. Tediosi, L. Tartara, and V. Degiorgio, "Dispersive wave generation by solitons in microstructured optical fibers," *Opt. Express* **12**, 124-135 (2004).
27. K. Sakamaki, M. Nakao, M. Naganuma, and M. Izutsu, "Soliton induced supercontinuum generation in photonic crystal fiber," *IEEE J. Sel. Top. Quantum Electron.* **10**, 876-884 (2004).
28. J. Teipel, K. Franke, D. Turke, F. Warken, D. Meiser, M. Leuschner, and H. Giessen, "Characteristics of supercontinuum generation in tapered fibers using femtosecond laser pulses," *Appl. Phys. B* **77**, 245-251 (2003).

## 1. Introduction

Recent advances in fiber technology have greatly facilitated the generation of supercontinuum radiation — the drastic spectral broadening of a laser pulse propagating in a nonlinear medium [1, 2]. Photonic crystal fibers [3, 4] and tapered fibers [5, 6] provide mode confinement, long interaction lengths, and customizable wavelength dispersion. These characteristics lead to octave-spanning supercontinuum generation in photonic crystal fibers [7]; and two-octave spanning wide spectra in tapered fibers [8].

By tapering photonic crystal fibers the interaction length required for supercontinuum generation can be reduced from meters [7, 8] to tens of millimeters [9, 10]. The resulting tapered photonic crystal fibers have submicrometer cores and outer fiber diameter on the order of tens of micrometers [9-11]. So, although photonic crystal fibers tightly confine light and present many advantages in robustness and isolation to environment, they are unsuitable for nanophotonic applications.

Recently, several groups reported the fabrication of low-loss silica submicrometer tapered fibers [10, 12, 13]. These nanophotonic waveguides have interesting linear optical properties [14] and give rise to supercontinuum generation with nanosecond and femtosecond pulsed lasers [9, 10].

According to theoretical models [15-17], the mechanism for supercontinuum generation by nanosecond and femtosecond laser pulses are different. For nanosecond pulses, stimulated Raman and parametric processes give rise to the broadening, while for femtosecond pulses self-phase modulation and four-wave mixing dominate. Experimentally supercontinuum generation in submicrometer fibers was demonstrated both with nanosecond [10] and femtosecond [9] pulses but only for fibers with diameter larger than 500 nm. Even though the mechanism for supercontinuum generation is very different for the two experiments, both report a sharp cut-off on the infrared side of the spectrum.

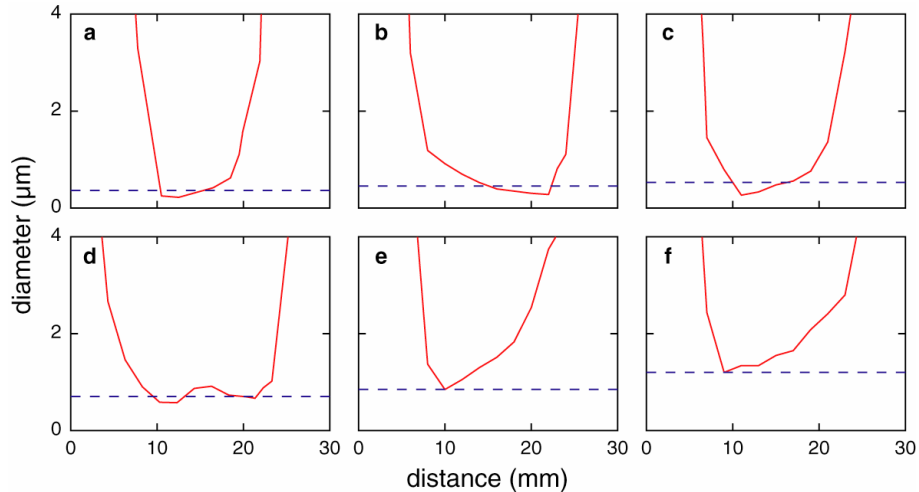


Fig. 1. Diameter profiles of six representative fibers. The average diameters of the submicrometer part of the fiber are: (a) 360 nm, (b) 445 nm, (c) 525 nm, (d) 700 nm, (e) 850 nm, (f) 1200 nm. The dashed horizontal lines mark the value of the average diameter.

In this letter, we report on supercontinuum generation by femtosecond laser pulses in silica fiber tapers with diameters as small as 90 nm. By varying the diameter from 90 nm to 1.6  $\mu\text{m}$  we can change the dispersion from normal to anomalous. We observe a strong diameter-dependence of the spectral broadening, which can be attributed to the fiber's diameter-dependent dispersion and nonlinearity. In the normal dispersion regime there is no sharp cut-off on the infrared side of the spectrum; in the anomalous dispersion regime we observe higher-order soliton formation and break-up.

## 2. Experimental

Several methods have been developed for fabricating submicrometer diameter silica wires [10, 12, 18, 19]. Initially we reported on a two-step drawing technique for fabricating nanowires with diameters down to 20 nm [12, 18]. In the experiments reported here, however, we use a conventional fiber tapering technique to produce low-loss submicrometer diameter wires that remain attached to a standard fiber on either side [10, 13].

The fiber pulling setup consists of a regulated hydrogen torch and two computer controlled linear stages. The parameters for the fiber pulling system, such as speed, acceleration, fiber tension and position of the flame, were optimized to yield relatively large lengths (tens of mm) of fibers of nearly constant diameter. We used a commercial 50  $\mu\text{m}$  core/125  $\mu\text{m}$  cladding multimode fiber as "preform" because the large mode area minimizes nonlinear effects outside the submicrometer part of the fiber. The diameter profile for each pulled fiber was measured using a scanning electron microscope.

To generate the supercontinuum spectra, we use femtosecond laser pulses with a central wavelength of 800 nm, a minimum pulse duration of 90 fs and maximum pulse energy of 4  $\mu\text{J}$ . Before reaching the submicrometer part of our fiber tapers, the laser pulse travels through a piece of standard fiber of about 150 mm length, which causes substantial dispersion of the laser pulse. We therefore adjust the dispersion of the input pulse using a grating compressor to compensate for the input fiber dispersion and shift the position of the shortest pulse to the submicrometer part of the fiber. Using this approach can deliver pulses as short as 200 fs at the output of a 150-mm long standard fiber.

For each fiber we first measured the low-intensity transmission at 800 nm (including coupling losses) using a photodiode. The supercontinuum spectra were recorded by coupling the output signal to a calibrated fiber-based spectrometer with a spectral range of 380 nm to 1050 nm. The spectra were time-averaged and recorded as a function of the input laser pulse

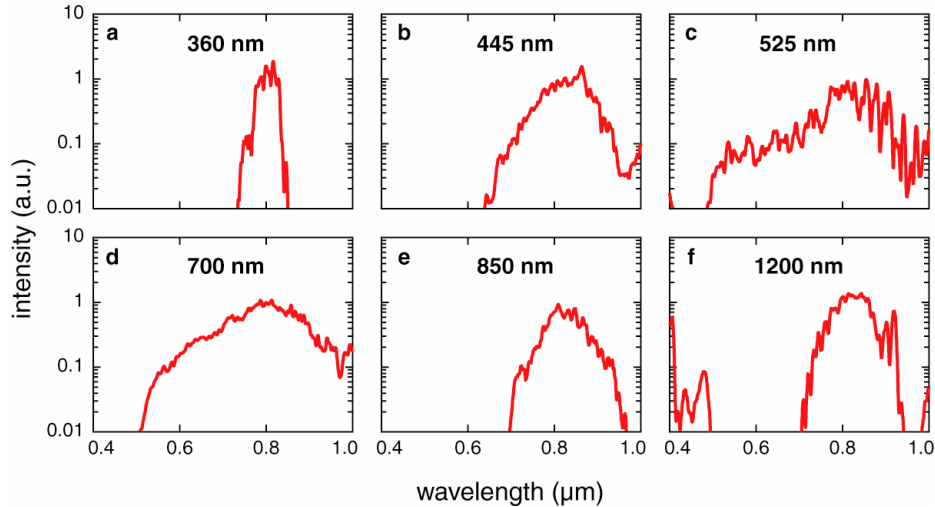


Fig. 2. Supercontinuum spectra for the six fibers of Fig. 1. The transmitted pulse energies are: (a) 0.3 nJ, (b) 4 nJ, (c) 6 nJ, (d) 4 nJ, (e) 7 nJ and (f) 2.5 nJ.

energy, up to the damage threshold of the fiber's front face (360 nJ).

### 3. Results

Figure 1 shows the diameter profiles of a number of representative fibers obtained from scanning electron microscope images. The dashed line marks the average diameter over the sub-1- $\mu\text{m}$  region of the tapered fibers (for fibers with larger diameters, this diameter is the minimum diameter). Although the six fibers shown have different interaction lengths and minimum diameters, we will, for simplicity, refer to each fiber by this average diameter.

Figure 1 also shows that the fibers are sharply tapered on either side and not necessarily symmetric. As in previously reported experiments [9], significant transmission losses occur at the taper region (about 70%). These losses can be reduced by using shallower tapers, but sharp tapers minimize the propagation length in the tapers region allowing us to neglect the contribution from the taper region to the supercontinuum spectrum.

Figure 2 shows the supercontinuum spectra obtained by transmitting a femtosecond laser pulse through each of the six fibers shown in Fig. 1. These spectra are representative of about 30 different spectra taken for fibers with average diameters ranging from 200 nm to 1600 nm.

The spectrum shown in Fig. 2(a) is representative of the spectra we obtain for fibers with average diameters from 200 nm to 400 nm. The small amount of broadening is independent of the input laser pulse energy. For fibers with average diameters below 300 nm the supercontinuum spectrum varies considerably in transmission and in the shape spectrum from one fiber to another. For these fibers typically less than 10% of the power is confined inside the fiber. The resulting large evanescent field is extremely sensitive to contamination of the surfaces [14], and so we can attribute the observed losses and spectral variance to surface contamination. When the losses are small, however, the spectrum is nearly identical to that shown in Fig. 2(a).

The supercontinuum spectrum becomes broader and more asymmetric with increasing average diameter between 400 nm and 700 nm [Figs. 2(b)-(d)]. The spectrum narrows again as the fiber diameter is increased from 700 nm to 1000 nm [Fig. 2(e)]. For average fiber diameters above 1000 nm, sharp peaks appear around 440 nm and in the near infrared [Fig. 2(f)].

Figure 3 shows the energy dependence of the output spectrum for the 1200-nm average diameter fiber in Fig. 2(f). At an input energy of 0.5 nJ we observe no broadening. As the input energy is increased, the spectrum broadens in the infrared and develops an increasing number of sharp features at 900 and 925 nm. At the highest energies sharp features also show

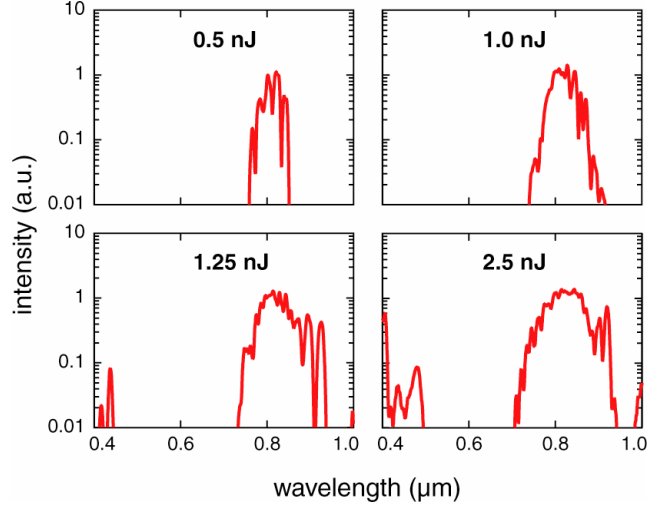


Fig. 3. Energy dependence of the supercontinuum spectrum generated by the 1200-nm minimum diameter fiber in Fig. 2(f).

up on of sharp features at 900 and 925 nm. At the highest energies sharp features also show up on the blue side at 415 and 437 nm.

#### 4. Discussion

Calculations of the nonlinearity  $\gamma$  of silica fibers with submicrometer diameters show that the nonlinear parameter is highly diameter-dependent and maximal for diameters of about 550 nm at a wavelength of 800 nm [20]. Figure 4 shows the diameter dependence of the dispersion coefficient  $D$  (dashed curve) and the nonlinearity  $\gamma$  (solid curve) for 800-nm light [14, 20]. The dispersion is negative (normal) for diameters smaller than 700 nm and positive (anomalous) for diameters between 700 nm and 1720 nm.

The broadening of the supercontinuum spectrum is due to an interplay between the nonlinearity and the dispersion of the fibers. Recently, several authors have clarified the complex propagation dynamics of femtosecond laser pulses inside fibers with varying diameter dependent dispersion and nonlinearity [21-23]. Qualitatively, however, we can estimate the relative contributions of the diameter dependent dispersion and nonlinearity to the supercontinuum spectra by comparing the length scales over which each effect occurs with the length of the fiber. The dispersion length  $L_D = -T_0^2 \lambda^2 / (2\pi c D)$  and the nonlinear length  $L_{NL} = T_0 \gamma^{-1} E_0^{-1}$  are shown in Table 1 for the pulse width  $T_0 = 200$  fs, the wavelength  $\lambda = 0.8$   $\mu\text{m}$ ,  $c$  the speed of light in vacuum, a pulse energy  $E_0 = 1$  nJ. In comparison, the part of the fibers that gives rise to the supercontinuum has an effective length  $L \approx 20$  mm (see Fig. 1).

Table 1. Physical parameters relevant to the propagation of intense 800-nm laser pulses in fibers with (sub)micrometer average diameters. The dispersion  $D$  is obtained from Ref. [14]; the effective nonlinearity  $\gamma$  from Ref. [20] and the dispersion length  $L_D$ , the nonlinear length  $L_{NL}$  and the soliton number  $N$  from Ref. [22]. The gray area marks the region of anomalous dispersion for 800-nm light.

diameter (nm)	$D$ (ps nm <sup>-1</sup> km <sup>-1</sup> )	$\gamma$ (W <sup>-1</sup> km <sup>-1</sup> )	$L_D$ (mm)	$L_{NL}$ (mm)	$N$
200	-370	2.5	260	400	
400	-3500	413	10	2.4	
600	-425	645	70	1.6	
800	160	500	190	2.0	9.6
1200	130	278	230	3.6	7.9

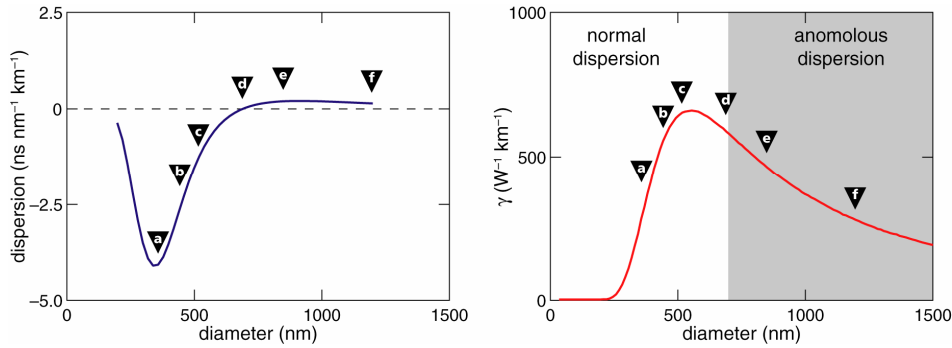


Fig. 4: Diameter dependence of the dispersion coefficient (dashed curve) and nonlinearity (solid curve) for 800-nm light. The dispersion  $D$  is obtained from Ref. [14]; the effective nonlinearity  $\gamma$  from Ref. [20]. The black triangles indicate the diameters of the fibers from Figs. 1 and 2.

For fibers with diameters ranging from 200 nm to 400 nm, the effective length of the fiber is smaller than the nonlinear length,  $L < L_{NL}$ , and so we expect little broadening, in agreement with our observations. For diameters around 400 nm, even though the nonlinearity is significant, the dispersion is very large and so the pulse stretches, reducing the intensity before any significant broadening occurs [see, *e.g.*, Fig. 2(a)].

The nonlinearity is largest for fiber diameters between 400 nm and 700 nm ( $L > L_{NL}$ ) giving rise to strong broadening in agreement with our observations [Figs. 2(b)–(d)]. It is interesting to compare the spectra for the two fibers with average diameters of 445 nm and 700 nm: although the nonlinearity  $\gamma$  is about the same for both fibers (Fig. 4), the spectral width is significantly different [Figs. 2(b) and 2(d)]. This difference is due to dispersion, which is an order of magnitude larger at a diameter of 445 nm than it is at a diameter of 700 nm (Fig. 4).

For diameters in the range 700–1000 nm, the nonlinearity is still high, but anomalous dispersion affects the generated spectrum. When the dimensionless number  $N = (L_D / L_{NL})^{1/2}$  is greater than one [22] solitons limit the broadening. As the values in Table 1 show,  $N$  is indeed significantly larger than one. For diameters above 1000 nm, the nonlinearity decreases significantly, while dispersion remains anomalous. In the anomalous dispersion regime, the spectra indeed show less broadening and the appearance of sharp soliton-like features [Figs. 2(e) and 2(f)]. The appearance of strong blue-shifted peaks at high fluence (Fig. 3) can be attributed to higher-order soliton self-splitting [23–28].

The spectra we observed for fiber diameters in the anomalous dispersion regime (diameter  $d > 700$  nm) differ from those observed in fibers of similar diameter with nanosecond pulses [10]. The supercontinuum generated with 532-nm nanosecond pulses has an almost flat, 300-nm wide spectrum [10], whereas the spectra generated with femtosecond pulses are not flat and about 200-nm wide [Figs. 2(e) and 2(f)]. Although at high energies solitons can give rise to a continuum of wavelengths [24–28], we are not able to achieve high enough intensities without damaging the fibers.

In previous work with femtosecond laser pulses in a tapered photonic crystal fiber with a core diameter of 550  $\mu\text{m}$ , a sharp cutoff observed at wavelengths above 850 nm is attributed to normal dispersion [9]. This cutoff, initially attributed to dispersion [9], was later attributed to wavelength dependent losses [21] caused by imperfections along the fiber. A direct comparison between this work and our results is difficult because it is unclear how to define the effective core size and interaction length of fibers. Nevertheless, the lack of a sharp cutoff in our spectra confirms that normal dispersion does not limit the infrared broadening of the supercontinuum spectrum.

From Table 1 we see that for fibers with diameters smaller than 200 nm, the effective length is an order of magnitude smaller than  $L_D$  and  $L_{NL}$ , and so nonlinear effects do not play a role in the pulse propagation. Although we don't have data for any fibers with average

diameters below 200 nm, fibers with minimum diameters below 200 nm show hardly any broadening, as one would expect. For such fibers more than 90% of the light is guided outside the silica core and so the effects of dispersion and nonlinearity are negligible. Consequently, a short pulse propagating in these fibers undergoes no spectral dispersion or broadening while still being guided by the fiber, suggesting that fibers with diameters smaller than 200 nm may be ideal for the guiding of intense, short pulses with minimal distortion.

## **5. Conclusion**

We observe supercontinuum generation of femtosecond laser pulses in silica fibers with average diameters ranging from 200 nm to 1600 nm and minimum diameters as small as 90 nm. The observed supercontinuum generation is due to an interplay between the diameter-dependent nonlinearity and the dispersion of the fiber. Because supercontinuum generation in submicrometer diameter fibers requires only a short interaction length (less than 20 mm) and low energy (1 nJ), such fibers are a promising source of coherent white-light for nanophotonics applications.

## **Acknowledgments**

Several people contributed to the work described in this paper. R. R. Gattass conceived of the basic idea for this work. R. R. Gattass and G. T. Svacha contributed equally to the experiment. Limin Tong participated in preliminary experiments and performed the numerical simulations. E. Mazur supervised the research and contributed to the manuscript. R. R. Gattass wrote the first draft of the manuscript; all authors subsequently took part in the revision process and approved the final copy. Tina Shih and Tommaso Baldacchini provided feedback on the manuscript throughout its development. The authors also would like to acknowledge the help of Mr. Xinyun Pan with the dispersion code. The research described in this paper is supported by the National Science Foundation under contracts PHY-0117795 and ECS-0601520. The authors would also like to acknowledge the use of facilities of the Center for Nanoscale Systems, which is supported by the National Science Foundation's National Nanotechnology Infrastructure Network.